ISSN 1063-7737, Astronomy Letters, 2007, Vol. 33, No. 12, pp. 844–847. © Pleiades Publishing, Inc., 2007.
Original Russian Text © B.A. Ioshpa, V.N. Obridko, V.E. Chertoprud, 2007, published in Pis'ma v Astronomicheskiĭ Zhurnal, 2007, Vol. 33, No. 12, pp. 941–945.

Small-Scale Stochastic Structure of the Solar Magnetic Field

B. A. Ioshpa[1*], V. N. Obridko[**], and V. E. Chertoprud

[1] *Pushkov Institute of Terrestrial Magnetism, Ionosphere, and Radiowave Propagation, Russian Academy of Sciences, Troitsk, Moscow oblast, 142190 Russia*

Received April 25, 2007

Abstract—The small-scale (∼10″) stochastic properties of the solar magnetic field B are analyzed in terms of the two-dimensional model of a fractal Brownian process (the mean square of the difference between the field strengths at two points separated by a distance D is proportional to D^{2H}). Digitized solar magnetograms with a 2″ resolution are used to determine the standard deviation s of the magnetic field and the exponents H at various levels of $|B|$. It has been established that the transition from the background magnetic field to the fields of an active region occurs near 25–50 G. A dependence of the exponent H on the magnetic field amplitude has been derived. The exponent H for the background magnetic field has been found to be much smaller than that for the fields of an active region. The relationship of the results obtained to certain fundamental properties of plasma in a magnetic field is discussed.

PACS numbers : 95.10.Ce
DOI: 10.1134/S1063773707120079

Key words: *Sun, solar magnetic fields, stochastic analysis.*

DATA PROCESSING

With the advent of digitized solar magnetograms with a ∼2″ resolution (the SOHO/MDI archive, everyday magnetic maps), it has become possible to study the small-scale (∼10″) stochastic properties of the solar magnetic field (Abramenko et al. 2002; Abramenko 2005; Nesme-Ribes et al. 1996; Salakhutdinova and Golovko 2005; Chumak 2005). Information about the structure of the solar magnetic field can be obtained by analyzing the dependence of the mean square of the difference between the magnetic field strengths at two points on the square of the distance between these points. We tested the two-dimensional model of a fractal Brownian process (Potapov 2005) to describe these properties. In this model, the variations in the solar magnetic field $B(x, y)$ at small distances $D = [(\Delta x^2 + \Delta y^2)]^{1/2}$ obey the relation

$$\langle [B(x,y) - B(x+\Delta x, y+\Delta y)]^2 \rangle \propto D^{2H}, \quad (1)$$

where the brackets $\langle\rangle$ denote averaging and the exponent H ($0 < H < 1$), which was called the Hurst exponent by Potapov (2005), characterizes the irregularity (roughness) of the $B(x, y)$ surface. (Below, we will not use this term lest H be confused with the classical Hurst exponent for the one-dimensional case.) The smaller the exponent H, the rougher the $B(x, y)$ surface. (The roughness itself can probably be interpreted as a manifestation of the hierarchy of magnetic flux tubes with various sizes.)

Finding the exponent H is reduced to calculating (using a magnetogram) the function $V(L) = \langle [B(x,y) - B(x+\Delta x, y+\Delta y)]^2 \rangle$ (where the averaging is performed over all Δx and Δy for which $\Delta x^2 + \Delta y^2 = L$) and to estimating the coefficient H in the regression equations

$$\log V(L) C + H \log L, \quad L \le L_M = d^2, \quad (2)$$

where C is a constant and d is the maximum scale used in finding H. Irrespective of the degree of accuracy of (1), the derived exponent is an independent characteristic of the small-scale structure. As will be shown below, this characteristic provides information about the temporal variations in the small-scale structure and about the distinctive features of this structure under various physical conditions. Varying the scale d, we can ascertain the distances D to which Eq. (1) holds. Estimates show that $D \sim 10''$–$20''$ for the small-scale field under study. Remarkably, in finding H, maps containing gaps in the $B(x, y)$ data can be processed; owing to this circumstance, the scheme used below works.

We analyzed the central region of the solar disk with latitudes $\phi = \pm 30°$ and longitudes $\lambda = \pm 30°$ displayed by a 499*499-pixel map. In addition to the

*E-mail: ioshpa@ttk.ru
**E-mail: obridko@izmiran.ru

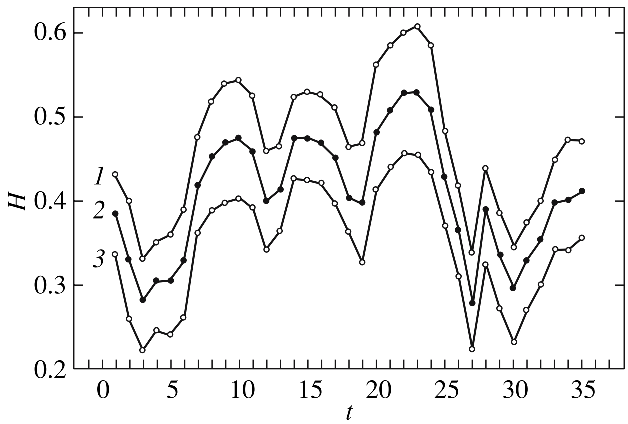

Fig. 1. Temporal variations in the exponent H. The H estimates were obtained at $d = 4''$ (*1*), $d = 10''$ (*2*), and $d = 19''$ (*3*) from the initial B data. The time is measured in days from July 6, 2002.

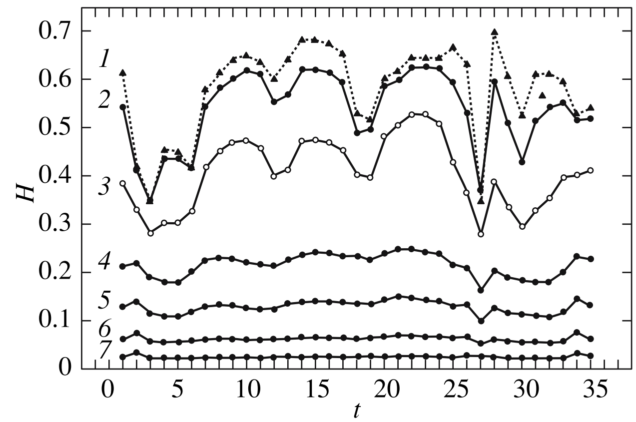

Fig. 2. Temporal variations in the exponent H obtained at various magnetic field levels: (*1*) $|B| \geq 50$ G, (*2*) $|B| \geq 25$ G, (*3*) $|B| \leq 2500$ G, (*4*) $|B| \leq 200$ G, (*5*) $|B| \leq 100$ G, (*6*) $|B| \leq 50$ G, (*7*) $|B| \leq 25$ G; $d = 10''$. The time is measured in days from July 6, 2002.

original map, we considered 18 modified versions in which the values of $|B|$ were bounded by one of the 18 levels (A or a) listed in (3); when the corresponding condition was violated, the value of $B(x, y)$ was replaced by a gap.

$$|B| \leq A, \quad A = 2000, 1500, 1000, 500, 200, 100, 50, 25, 10, 5, 3 \text{ G};$$
$$|B| \geq a, \quad a = 25, 50, 100, 150, 200, 250, 300 \text{ G}.$$

The data of the original (unmodified) map are subject to the condition $|B| \leq A$, $A = 2500$ G. For 19 versions of the map under consideration, we determined the standard deviations s of the magnetic field and the exponents H (six estimates in each version with different values of d, from $4''$ to $24''$). Using the described scheme, we processed all magnetograms of the day under consideration (except for the nonstandard, averaged magnetograms marked in the SOHO/MDI archive by an asterisk) and calculated the daily mean s and H, which formed the basis for the subsequent analysis.

To study the temporal variations in H, we chose a 35-day interval (from July 7 through August 10, 2002) with dramatic changes in solar activity and three days with weak activity (February 13, May 8 and 14, 2006) and processed 405 magnetograms pertaining to these days. The chosen 35-day interval was characterized by dramatic changes in $F_{10.7}$, from 133 to 249, and by the presence of large-scale magnetic fields of three regions with a strong field in the map. On these three days with weak activity, $F_{10.7}$ was 74, 86, and 74 respectively.

RESULTS

Figure 1 gives an idea of the variations in the exponent H in a time interval exceeding one solar rotation. The H estimates were obtained from the original (unmodified) maps for three values of the maximum scale d ($4''$, $10''$, and $19''$). As can be seen from the plots in Fig. 1 and is confirmed by our calculations for all six values of d, the $B(x, y)$ surface on small scales is not perfectly fractal: as the maximum scale d increases from $4''$ to $24''$, the mean value of H does not remain constant, but decreases by a factor of 1.5, from 0.46 to 0.31. Thus, the roughness of the $B(x, y)$ surface increases with d and this may be a manifestation of the hierarchy of magnetic structures.

The relative variations in the exponent H calculated at different values of d are almost the same (in all cases, the H variability coefficient is close to 0.2, while the minimum correlation coefficient between the H variations obtained for different values of d is 0.97). Therefore, in what follows, we will discuss the results pertaining to one level, $d = 10''$.

The H variations themselves, as their comparison with the map of the large-scale magnetic field shows, are related to the solar rotation and to the passage of active regions through the central meridian. Higher values of H correspond to stronger magnetic fields. A similar conclusion can be drawn from an examination of Fig. 2, which shows the H variations at various magnetic field levels (7 of the 19 calculated versions are displayed). The increase in H with $|B|$ is accompanied by two peculiarities. First, this increase virtually ceases when going from the $a = 25$ G level to the $a = 50$ G level and further. Second, the H

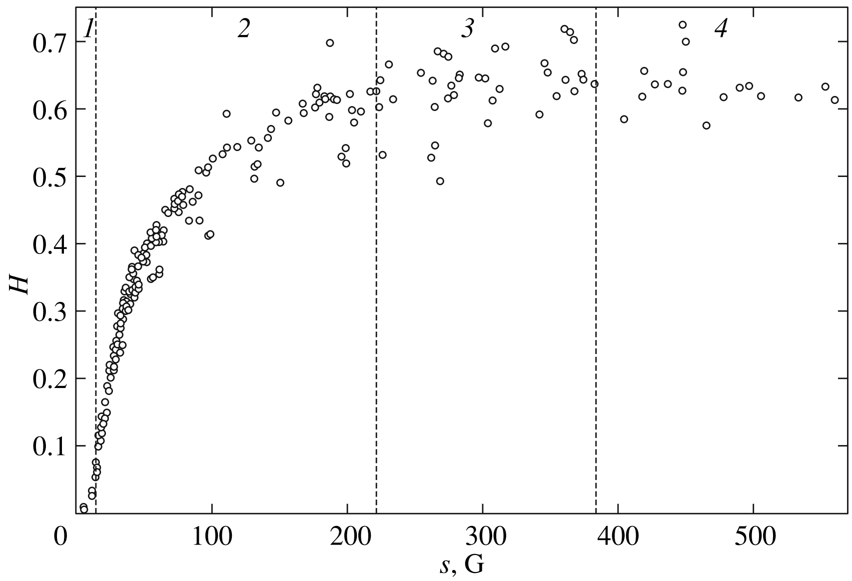

Fig. 3. Dependence $H(s)$ derived from the data of a 35-day interval at $d = 10''$: (*1*) $|B| \leq 50$ G; (*2*) 2 G $\leq |B| \leq 2500$ G; (*3*) $|B| \geq 50$ G; (*4*) $|B| \geq 150$ G.

variations observed at high $|B|$ levels that are related to the passage of active regions through the central meridian are traceable to low levels, disappearing at $A = 25$ G. The graphic information is confirmed by our correlation analysis of 19 versions of the $H(t)$ curves (in particular, the correlation coefficient between H for $|B| \leq 100$ G and $|B| \geq 100$ G is 0.54). These peculiarities in the H variations suggest that the division between the background and an active region takes place at a level of 25–50 G.

The daily means of the standard deviation s of the magnetic field and the exponent H obtained for 19 versions and 35 days allow us to construct the dependence $H(s)$ of the exponent H on the magnetic field amplitude. In constructing this dependence, we checked the reliability of the H estimates. An H estimate was rejected as unreliable if $H_{10}/H_{14} \geq 1.3$, where H_m is the H estimate at $d = m''$.

Figure 3 presents the dependence $H(s)$, which includes about 500 points. For the convenience of interpretation, we selected four areas in Fig. 3 with different conditions imposed on the analyzed magnetic fields. In area *1* (i.e., at $s \leq 16$ G), $|B| \leq 50$ G; in area *3*, $|B| \geq 50$ G; in area *4*, $|B| \geq 150$ G; and in area *2*, any values 2 G $\leq |B| \leq 2500$ G are possible, but weak fields dominate. Area *1* pertains to the background magnetic field, while areas *3* and *4* pertain to the magnetic fields of an active region. In area *2*, a *mixture* of the magnetic fields of the background and active regions is analyzed and intermediate results are obtained. The standard deviation s gives a idea of the characteristic strength of the magnetic field under study.

As follows from the estimates of Fig. 3, the exponent H is 0.5–0.7 for the magnetic fields of an active region and ∼0.1 for the background field. Two more circumstances are remarkable. There is no significant dependence on the field amplitude in the H estimates for the magnetic fields of an active region and the estimates themselves are limited by 0.75. Thus, when going from the background magnetic field to the fields of an active region, the roughness of the $B(x, y)$ surface decreases, but does not disappear.

To improve the H estimates for the background magnetic field, we analyzed the magnetograms obtained for days with weak solar activity (February 13, May 8 and 14, 2006). Figure 4 presents the $H(s)$ estimates for seven versions: (*1*) $|B| \leq 5$ G, (*2*) $|B| \leq 10$ G, (*3*) $|B| \leq 25$ G, (*4*) $|B| \leq 50$ G, (*5*) $|B| \leq 100$ G, (*6*) $|B| \leq 200$ G, (*7*) $|B| \leq 500$ G. Three estimates are given for each version (there are fewer points where the estimates coincide).

Using a series of 13–14 H estimates for one quiet day and determining the standard deviation of H in this series, we can get an idea of the upper limit on the error in H. For $|B| \leq 25$ G and for each of the three days, this value does exceed 0.0006. The error for the daily mean estimate of H is a factor of 2–3 smaller. This error is many times smaller than the standard deviation of $H(t)$ on curve *7* of Fig. 3, which is 0.0024. Thus, for $|B| \leq 25$ G, the H variations are considerably higher than the errors in H and the absence of a correlation between the H variations for weak and strong magnetic fields is not caused by the level of errors in H.

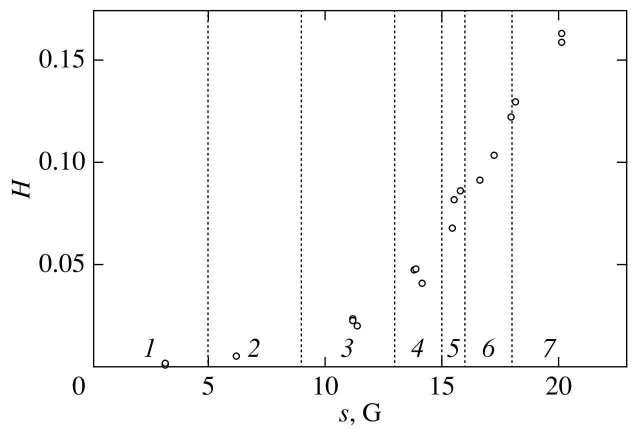

Fig. 4. Dependence $H(s)$ obtained from the data of three quiet days in 2006 at $d = 10''$: (*1*) $|B| \leq 5$ G; (*2*) $|B| \leq 10$ G; (*3*) $|B| \leq 25$ G; (*4*) $|B| \leq 50$ G; (*5*) $|B| \leq 100$ G; (*6*) $|B| \leq 200$ G; (*7*) $|B| \leq 500$ G.

The background dependences $H(s)$ shown in Figs. 3 and 4 for the quiet and active Sun are in good agreement. Thus, the presence of active regions on the Sun probably does not affect noticeably the small-scale structure of the background magnetic field. The data presented in Fig. 4 illustrate the stability of the H and s estimates when passing from one quiet day to another. The kink in the dependence $H(s)$ at $s \approx 10$ G may be related to the fact that the level of errors that should be ~6 G in this case is reached.

CONCLUSIONS

Using the exponent H to describe the evolution of the small-scale structure of the solar magnetic field allowed us to reveal changes in this structure with changing physical conditions. At relatively weak fields, the magnetic field suppresses the turbulent friction, causing the convective heating to be enhanced. This is how a photospheric facula arises (Pikel'ner 1960). The required characteristic fields can be easily estimated from the ratio of the magnetic and kinetic energies. These energies are comparable if the parameter

$$\beta = \frac{B}{V\sqrt{4\pi\rho}}, \tag{3}$$

where B is the magnetic field strength, V is the kinetic velocity, and ρ is the density, is close to 1. For our estimate, assuming that $\rho \sim 3 \times 10^{-8}$ cm^{-3} and $v \sim 10^5$ cm s^{-1} at the level of $\tau \sim 0.1$ where the strong Fraunhofer lines originate, we will obtain $B \sim 60$ G. Since the suppression of turbulence begins at β slightly lower than unity, we may assume that our conclusion that the magnetic field begins to smooth its distribution at 25–50 G is in good agreement with the theoretical estimates.

Approximately the same magnetic field strength is believed to be characteristic of the boundaries of calcium flocculi (Stepanov and Petrova 1959). However, since the density is much lower at the CaII emission level, we may assume that our estimation will give an even lower value.

As the field strength increases to several hundred gauss, the magnetic field begins to suppress the convection. In the presence of a magnetic field, the standard condition for convective instability $\nabla/\nabla_{\rm ad}$ is replaced by a different one:

$$\frac{B^2}{B^2 + 8\pi P} < \nabla - \nabla_{\rm ad}, \tag{4}$$

where ∇ is the mean temperature gradient in the medium $d\log T/d\log P_{\rm g}$, $\nabla_{\rm ad}$ is the adiabatic gradient equal to 0.4, and $P_{\rm g}$ is the gas pressure. For instance, the gradient in sunspots exceeds only slightly the adiabatic one (Obridko 1985); therefore, the right-hand side of Eq. (5) is less than 0.1 (Zwaan 1975). At $P_{\rm g} \sim 10^5$, we will obtain the boundary value for $B \sim 500$ G. Since area *4* in Fig. 3 is defined by the condition $|B| \geq 150$ G, we may assume that the flat part in Fig. 3 means the region of suppressed convection. Once this boundary has been reached, the further "smoothing" ceases or slows down greatly.

ACKNOWLEDGMENTS

We wish to thank the creators of the SOHO/MDI archive. This work was supported by the Russian Foundation for Basic Research (project nos. 07-02-00333 and 07-02-00246).

REFERENCES

1. V. I. Abramenko, V. B. Yurchyshyn, H. Wang, et al., Astrophys. J. **577**, 487 (2002).
2. V. I. Abramenko, Sol. Phys. **228**, 29 (2005).
3. Archive SOHO/MDI, Everyday Magnetic Maps.
4. O. Chumak, Astron. Astrophys. Trans. **24**, 93 (2005).
5. E. Nesme-Ribes, N. Meuner, and D. Collin, Astron. Astrophys. **308**, 213 (1996).
6. V. N. Obridko, *Sunspots and Complexes of Solar Activity* (Nauka, Moscow, 1985) [in Russian].
7. S. B. Pikel'ner, Astron. Zh. **37**, 616 (1960) [Sov. Astron. **37**, 590 (1961)].
8. A. A. Potapov, *Fractals in Radiophysics and Radar: Sampling Topology* (Universitetskaya Kniga, Moscow, 2005), p. 463.
9. I. L. Salakhutdinova and A. A. Golovko, Sol. Phys. **225**, 59 (2005).
10. V. E. Stepanov and N. N. Petrova, Izv. Krymsk. Astrofiz. Obs. **21**, 152 (1959).
11. C. Zwaan, Sol. Phys. **45**, 115 (1975).

Translated by G. Rudnitskii